
MACHINE LEARNING OF NONEQUILIBRIUM PHASE TRANSITION IN AN ISING MODEL ON SQUARE LATTICE

A PREPRINT

Dagne Wordofa
 Department of Physics
 Addis Ababa University
 Addis Ababa, Ethiopia
 dagnehordofa@gmail.com

Mulugeta Bekele*
 Department of Physics
 Addis Ababa University
 Addis Ababa, Ethiopia
 mulugetabekele1@gmail.com

July 25, 2023

ABSTRACT

This paper presents the investigation of convolutional neural network (CNN) prediction successfully recognizing the temperature of the non-equilibrium phases and phase transitions in two-dimensional (2D) Ising spins on square-lattice. The model uses image snapshots of ferromagnetic 2D spin configurations as an input shape to provide the average out put predictions. By considering supervised machine learning techniques, we perform the (modified) Metropolis Monte Carlo (MC) simulations to generate the equilibrium (and non-equilibrium) configurations. In equilibrium Ising model, the Metropolis algorithm respects detailed balance condition (DBC), while its modified non-equilibrium version violates the DBC. Violating the DBC of the algorithm is characterized by a parameter $-8 < \varepsilon < 8$. We find the exact result of the transition temperature in terms of ε . This solution is used to encode the two (high-and low-temperature) phases through an order parameter of the model. If we set $\varepsilon = 0$, the usual single spin flip algorithm can be restored and the equilibrium configurations (training dataset) generated with such set up are used to train our model. For $\varepsilon \neq 0$, the system attains the non-equilibrium steady states (NESS), and the modified algorithm generates NESS configurations (test dataset), not defined by Boltzmann distribution. Finally, the trained model has been validated and successfully tested on the test dataset. Our result shows that CNN can correctly determine the nonequilibrium phase transition temperature T_c for various ε values, consistent with the exact result (our study) and also in agreement with MC result (literature).

Keywords Non-equilibrium, Phase Transition, Ising, Critical Temperature, Machine Learning

1 Introduction

Currently, the standard theory and general framework for the critical phenomenon near continues phase transitions (PT) is well understood in equilibrium systems [1–3]. However, the study of phase transitions between non-equilibrium statistical states have consistently been among the main subjects of ongoing research and exploration [4–11]. Identifying the critical points of various phases within the parameter space is a fundamental undertaking in the fields of statistical and condensed-matter physics. Machine learning (ML) is the field of study concerned with algorithms that are designed to improve their performance by getting experience from data [12]. Relatively recently, the utilization of these techniques have been successfully employed in various domains such as investigating the phases of the Ising model [13–16], phase transition in the Bose-Hubbard [17, 18], disordered quantum systems [19, 20], and material properties [21].

In this report, we introduce the application of ML to non-equilibrium PT which can be accomplished based on the well established features of modern theories of PT in equilibrium systems. In equilibrium systems, PT is generically

*Corresponding author

described by singularities in the free energy and its derivatives. Such singularity causes a discontinuous property of thermodynamic quantities near the transition point. Phenomenologically, the PT is defined regarding to an *order parameter*, which has a zero value in the ordered phase while it vanishes in the disordered phase [22–24]. Within the scope of this paper, the paradigmatic example that we will be working on is a two-dimensional (2D) Ising spin system on a square lattice. It is interesting to note that the 2D Ising spin on square-lattice is a simple that can be exactly solved [22]. Despite the fact that it is exactly solvable, it is still a topic of ongoing research that is frequently used in the context of ML [13–16, 25–32]. In this investigation, first we try to perform the graphical solution (7) of the nonequilibrium transition temperature, see supplementary page A.1. Then we look at the possibility of a non-equilibrium phase transitions occurring within the Ising model that breaks the principle of detailed balance through machine learning. To be more explicit, we aim to find the non-equilibrium phases and the transition temperatures by applying convolutional neural networks (CNN) based on the general framework of supervised learning discussed in [33]. This framework was reviewed before in Statistical Mechanics of deep learning, which also briefly explain the connection between deep learning and the modern subject of Statistical Physics.

According to the findings presented in Ref. [28], the application of ML to the issue of phases of matter has, for the most part, been effective, and motivated with this work, we aim to extend this ML application to the case of *non-equilibrium* PT in 2D Ising model. For its compatibility, the Ising model which was addressed in [34] becomes the primary focus of our attention. We employ the Monte Carlo (MC) approach [35–38] to generate a properly distributed data set of Ising spin configurations on $L \times L$ square lattice (where L is its leaner size), together with their associated labels, while taking supervised learning techniques into consideration. Accordingly, by the context of equilibrium and non-equilibrium systems, we are referring to two different spin update rules; (i) rule that holds the DBC and (ii) rule that breaks the DBC, respectively. The former is used to generate the *train-dataset*, while the latter is used to generate the *test-dataset* which can be seen from some representative configurations illustrated in A.2 (Figure 4).

We build a CNN using open-source software [39], see supplementary information (A.3) and an example shown in Figure 7 for more details. We train our model on the train-dataset and it has been effectively validated to classify simulation results of the equilibrium 2D Ising model into the ferromagnetic (FM) or "ordered state" and the paramagnetic (PM) or "disordered state" phases. The classification of these results was also successfully validated, for example [28, 29]. The main goal of this work is to evaluate the generalization reach of the CNN by testing it with configurations (test-dataset) from a system that is not in equilibrium. Intriguingly, in addition to accurately categorizing the configurations, we will demonstrate that the CNN can exhibit the critical temperature of the non-equilibrium PT. Our findings is very close to the exact solution (7), and also consistent with the MC results provided in Ref. [34].

The remaining sections are organized as follows: Next, we present the model considered in this research, followed by a concise description of the Metropolis MC method for generating image samples of Ising configurations in Section 2. Some of the results of this study are then illustrated in Sec. 3. Finally, we provide a summary of the main results and discussion as presented in Sec. 4.

2 Description of the Model and Metropolis Monte Carlo Method

We consider the 2D Ising model on a square lattice of linear size L sites. The system size ($\mathcal{N} = L \times L$) is equal to the total number of spins (N), which means that each of the site contains one spin that points either up or down (± 1). If we assume zero magnetic field, the nearest-neighbor interaction energy of (ferromagnetic) Ising model is given as,

$$E = -J \sum_{\langle i,j \rangle} \sigma_i \sigma_j, \quad (1)$$

where $\sigma_i = \pm 1$ denotes the value of the spin at site $i = \{1, \dots, \mathcal{N}\}$, the indices $\langle i, j \rangle$ represent the nearest-neighbor pairs [35, 36], and a ferromagnetic energy scale $J > 0$ refers to the strength of exchange interaction.

At the critical (or transition) temperature, the system exhibits a second order phase transposition. The transition temperature of the nearest-neighbor equilibrium Ising model, for an infinite square lattice, was derived [22] to be $2/\ln(1 + \sqrt{2})$, see Eq. (6). In this case, the system is assumed as a *magnetized state* when its temperature is lower than $2/\ln(1 + \sqrt{2})$, which is known as the ordered state (FM phase). On the other hand, the system is said to be in the disordered state (PM phase) if its temperature is higher than $2/\ln(1 + \sqrt{2})$. The magnetization per spin is what determines the value of the order parameter,

$$m = \frac{1}{N} \left| \sum_i^N \sigma_i \right|. \quad (2)$$

This quantity (2) distinguishes the *two phases* that are realized by the system. It is zero(nonzero) in the disordered(ordered) phase.

2.1 The Modified Metropolis Algorithm

Let us consider a system that is in contact with a heat bath and produces stochastic spin flips, following Ref. [41]. In the context of the equilibrium Ising model, it can be observed that the system attains thermal equilibrium over a significant time and thus the steady state distribution can be accurately described by the Boltzmann distribution. This is a valuable approach for establishing transition rates and calculating the probabilities of spin flipping. The Metropolis algorithm [37] is the transition rate that is commonly used and can be stated as

$$W = \text{MIN} \left[1, e^{-\Delta E / k_B T} \right], \quad (3)$$

where W represents the rate of change from state b (*before* flip) to another state a (*after* flip), $\Delta E = E_a - E_b$ is the change in energy that occurs as a result of this transition, and k_B denotes the known Boltzmann's constant. In this context, the unit of temperature T is linked to the units of J/k_B . (For the remainder of this description, we will assume $k_B = 1$, thus $T = T/J$ becomes dimensionless.) The defined algorithm (3) meets the requirements of the detailed balance condition (DBC). The aforementioned statement denotes that there exists a microscopic reversibility of every elementary process, which is counterbalanced by its corresponding reverse process [42]. That is $W_{b \rightarrow a} p_{eq}^b = W_{a \rightarrow b} p_{eq}^a$, where $p_{eq}^b \propto \exp[-E_b/T]$. Therefore the ratio $w = W_{b \rightarrow a}/W_{a \rightarrow b}$ gives $w = \exp[-\Delta E/T]$.

The topic of non-equilibrium phase transitions is examined with emphasis on fundamental characteristics such as the role of DBC violation in generating effective (long-range) interactions [33]. The equilibration process is not solely dependent on the presence of DBC, as it serves as a sufficient but not a necessary condition. The objective of this study is to deliberately violate the DBC in order to induce a state of *fluctuation* in the system. As noted in reference [34], there exists a scenario in which the system undergoes an order-disorder phase transitions that different from the typical transitions of the equilibrium case. If $\varepsilon \neq 0$ denotes the parameter violating the DBC, it is possible to substitute ΔE in Eq. (3) with

$$\Delta E_{\text{eff}} = \Delta E + \varepsilon, \quad (4)$$

and the ratio becomes $w = e^{-\beta(\Delta E + \varepsilon)}$. It can be inferred that when ε is positive, ΔE_{eff} is greater than ΔE , whereas when ε is negative, ΔE_{eff} is less than ΔE . The former does not facilitate the process of spin flipping, whereas the latter significantly promotes the likelihood of spin flipping. In contrast to spins subjected to the conventional Metropolis algorithm (3), spins subjected to the modified flipping rates effectively undergo distinct (transition) temperatures. When $\varepsilon < 0$ ($\varepsilon > 0$), it is reasonable to assume that the spins are coupled to a reservoir at a higher (lower) effective temperature (T_{eff}). It should be noted that T_{eff} is not uniform across all spins in the system, see appendix A.1. Thus, “the system is out-of-equilibrium, and a transition is a non-equilibrium phase transition. The property of this transition would be a characteristic of the *non-equilibrium steady statey* (NESS) exhibited by the system” [34]. It can be inferred that, unlike an equilibrium system, the distribution of microstates in the NESS cannot be characterized by the Boltzmann distribution. The transition rate for flipping a spin $\sigma_i^b \rightarrow \sigma_i^a$ can be determined using this definition (4),

$$W(\pm \sigma_i \rightarrow \mp \sigma_i) = \begin{cases} e^{-\beta(\varepsilon \pm \Delta E)}, & \text{if } \varepsilon \pm \Delta E > 0; \\ 1, & \text{otherwise.} \end{cases} \quad (5)$$

Here $\Delta E = 2J\sigma_i \sum_j \sigma_{ij} \equiv \{-8, -4, 0, 4, 8\}[J]$ where σ_{ij} refers to $j = \{\text{left, right, top, bottom}\}$ nearest neighbors of the i^{th} site, and the symbol ‘ \equiv ’ refers to an alternative approach for Ising on a square lattice involves that ΔE can assume discrete values from $\{-8, -4, 0, 4, 8\}$ using the units of J . The algorithm given in Eq. (5) still respects the DBC when $|\varepsilon| \geq 8$ [43]. Intriguingly, however, algorithm (5) violates the DBC for $-8 < \varepsilon < 8$ (with $\varepsilon \neq 0$) since it is impractical to obtain a unique T_{eff} value for which the transition probabilities for all feasible ΔE values that obey the DBC. According to the established notation, the non-equilibrium phase transitions may occur within the system and the transition temperature T_c must fulfil the relation,

$$T_c = \begin{cases} 0 < T_c < T_c^0 & \text{if } -8 < \varepsilon < 0; \\ T_c^0 < T_c < 2T_c^0 & \text{if } 0 < \varepsilon < 8, \end{cases} \quad (6)$$

where $T_c^0 = 2/\ln(1 + \sqrt{2}) \approx 2.2692$ is the transition temperature of the *equilibrium* ($\varepsilon = 0$) case. Explicitly, we are essentially interested in some ε values of $-8 < \varepsilon < 8$, as shown in Figure 1. Referring to a systematic graphical solution presented in (A.1) the exact result follows that,

$$T_c^{\text{exact}}(\varepsilon) \equiv T_c = \begin{cases} (0.5 + \varepsilon/16)T_c^0, & \text{for } -8 < \varepsilon < -4; \\ (1 + 3\varepsilon/16)T_c^0, & \text{» } -4 \leq \varepsilon \leq 4; \\ (1.5 + \varepsilon/16)T_c^0, & \text{» } 4 < \varepsilon < 8, \end{cases} \quad (7)$$

where $T_c^0 \equiv T_c(\varepsilon = 0) = 2/\ln(1 + \sqrt{2})$, see Figure 1. Specifically, if we focus on $-4 \leq \varepsilon \leq 4$ that Eq. (7) can be efficient to discuss the nonequilibrium phase transition. More specifically, consider two ε values ($\varepsilon = \pm 2$), conveniently we get that $T_c^{\text{exact}}(\varepsilon = \pm 2) \approx 3.1201 (\approx 1.4182)$. Remarkably, we see that our numerical result (Figure 3) is very close to this result.

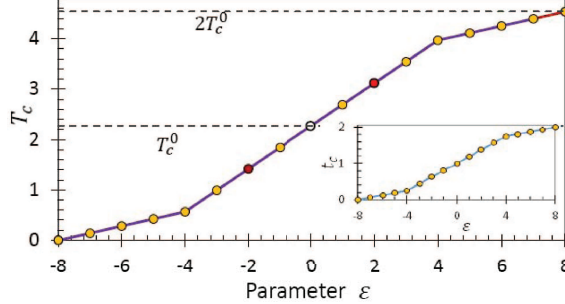


Figure 1: Transition temperature T_c as a function of parameter ε . A Plot of Eq. (7). The horizontal dashed lines represents $T_c = T_c^0$ and $T_c = 2T_c^0$ as shown where $T_c^0 = 2/\ln(1 + \sqrt{2})$. The inset shows t_c versus ε where $t_c = T_c/T_c^0$.

2.2 Generating 2D Images of Ising Spin Configurations

Make use of the modified Metropolis rule (5), we achieve Monte Carlo (MC) simulations of the Ising model, see the flow chart shown in A.2 (Figure 5). The simulations are performed on a square lattice ($L_x = L_y$) of system size $\mathcal{N} = L^2$, inducing periodic boundary condition in (x and y) directions. For each system, we start the simulations from an initial, high temperature (with random spin initial configurations) and perform a standard MC sweeps (MCS) for generating the required samples of $L \times L$ Ising spin configurations as data for the supervised ML approach [35–38]. Examples of configurations are shown in Figure 6. For all datasets used in Sec. 3, the simulation was performed with three $\varepsilon = \{0, 2, -2\}$ values. First we set $\varepsilon = 0$ and generate the configurations for the train-dataset. This comprises about 80% of the total data (where 10% is again reserved for validation). Next we set $\varepsilon = 2$ to generate the test-dataset which incorporates the remaining 20% of the total data, and the procedure is the same for $\varepsilon = -2$. We restart and repeat this procedure for all system sizes. Furthermore, one can save the trained sequential model using TensorFlow’s Keras API, and later it can be loaded to test the configurations from different discrete ε values. Efficiently, this can be used to study the qualitative dependence of T_c on the parameter ε , e.g., see A.4.

3 Results

In the current section (Sec. 3), we briefly present the main numerical results obtained using neural network model (CNN). Similar to the previous works (literatures), we train the model on equilibrium Ising spin configuration. After training on an adequately large sample size at temperatures $T > T_c^0$ and $T < T_c^0$, the CNN can correctly classify configurations in a valid dataset, as illustrated in Figure 2(a) for configurations with the given linear size, $L = \{10, 20, 40, 60\}$. Systematically, finite-size scaling (FSS) is capable of narrowing on the thermodynamic result

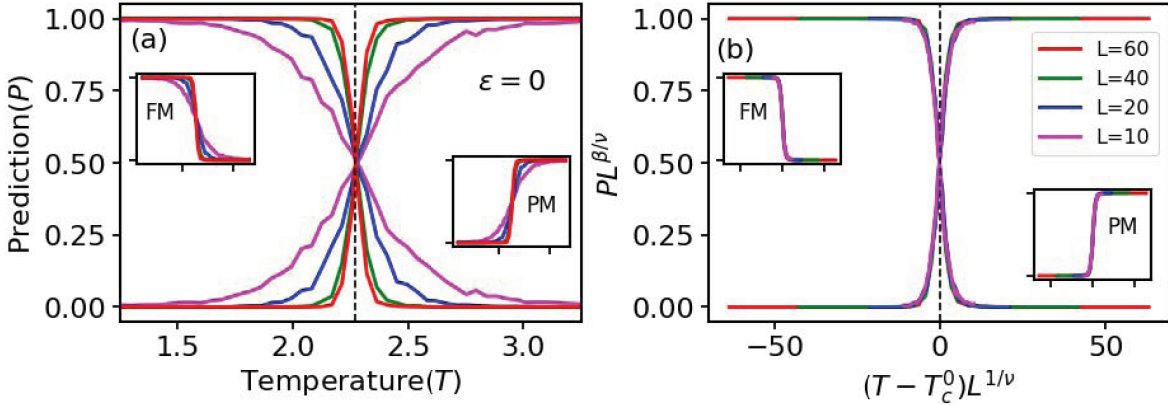


Figure 2: Machine learning (ML) the *equilibrium* ($\varepsilon = 0$) ferromagnetic Ising spin on square-lattice (linear sizes $L = 10, 20, 40$ and 60). (a) The prediction P versus temperature T where the vertical dashed line denotes the estimated value of $T_c^0 \simeq 2.2687 \pm 0.0015$ of the model. (b) A plot showing data collapse of $PL^{\beta/\nu}$ versus $(T - T_c^0)L^{1/\nu}$. The insets represent FM curves and PM curves as shown.

of T_c^0 in a manner comparable to that of magnetization [28], Figure 2b displays that a data collapse yields a critical

exponents estimate of $\nu \approx 1.00 \pm 0.01$ and $\beta \approx 0.125 \pm 0.002$, while a size scaling of the crossing temperature yields an estimate of $T_c^0 \simeq 2.269$ (see A.5).

More interestingly, “the generalization competency of the neural networks lies in their ability to provide correct predictions further than the datasets with which they were trained”. Accordingly, the trained CNN has been provided with a test dataset of configurations from a 2D Ising model in which data generation was incorporated by changing the update rules where violation of the DBC is accountable. This is intended to answer the question “*Does CNN that trained on equilibrium phase transition in Ising model with detailed balance able to recognise the non-equilibrium phase transition?*” Thus, next we present the results of this scenario by using our CNN, which is already trained and validated on configurations for the square-lattice ferromagnetic Ising model, and provide it a test dataset generated by modified Metropolis MC simulations for the same sizes as L s in Figure 2. In Figure 3 we illustrate the average of

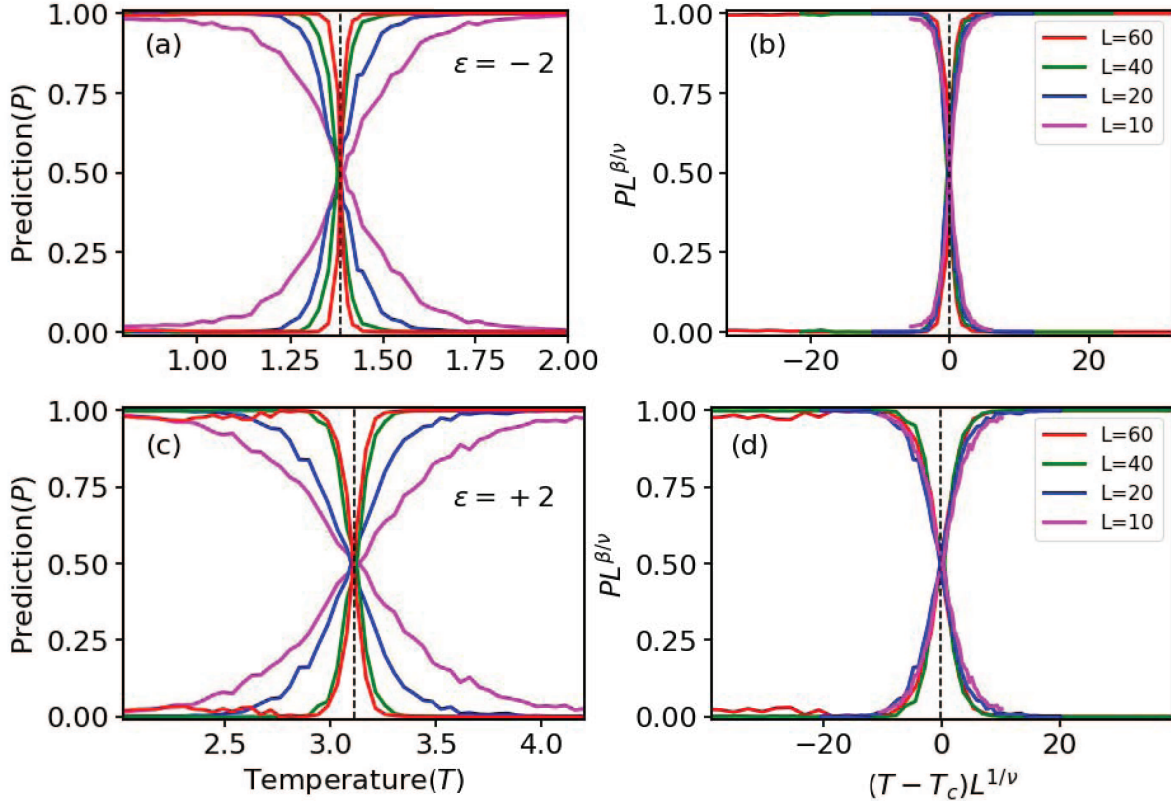


Figure 3: ML the non-equilibrium ($\varepsilon \neq 0$) ferromagnetic Ising spin on square-lattice ($L = 10, 20, 40$ and 60) where $\varepsilon = -2$ (a) and $\varepsilon = +2$ (c). The left panel (a and c) display P versus T while the right panel (b and d) represent the corresponding data collapse $PL^{\beta/\nu}$ versus $(T - T_c)L^{1/\nu}$. The estimated values are indicated by dashed lines: $T_c \simeq 1.3769 \pm 0.0087$ (a), and $T_c \simeq 3.1071 \pm 0.0175$ (c)

prediction P versus temperature T for configurations from two different test datasets ($\varepsilon = \pm 2$) of each with four linear sizes (see keys). The dashed lines denote the estimated values of the transition temperatures (a) $T_c \simeq 1.377$, and (c) $T_c \simeq 3.107$. Clearly we see that $T_c^{\text{ML}}(\varepsilon = \pm 2)$ is close to $T_c^{\text{exact}}(\varepsilon = \pm 2)$ obtained in Eq. (7). On the right panel, ‘b’ and ‘d’ represent the corresponding data collapse $PL^{\beta/\nu}$ versus $(T - T_c)L^{1/\nu}$ allowing us to successfully compute the critical exponents, $\nu \approx 1.02 \pm 0.02$ and $\beta \approx 0.126 \pm 0.003$. Our results are consistent with the MC result reported in [34].

4 Summary and Conclusions

In order to categorize the two typical phases of ferromagnetic Ising spins on square-lattice, we used supervised machine learning approaches. Our findings indicate that advanced ML architectures, such as the fully connected CNN, are able to detect non-equilibrium transition temperature T_c so long as they are properly trained on equilibrium Ising spin configurations. To train (and validate) the model, we use the training dataset generated by running the MC

simulations of 2D ferromagnetic Ising system on square-lattice, where the spin's update rule is governed by the usual Metropolis algorithm. This update rule is compliant with the DBC. Then we test the model on simulations of 2D ferromagnetic system (test dataset) and, in this case, the update scheme is performed using modified version of the algorithm. That is; the modified update rule violates the DBC. In the model, violating DBC is designated by a parameter ϵ that is fixed to take values in the range $-8 < \epsilon < 8$. We successfully derived the exact solution of the non-equilibrium transition temperature $T_c(\epsilon)$, Eq. (7). This solution suggests that only the parameter ϵ affects the transition temperature. For $\epsilon = 0$, the equilibrium transition T_c^0 can be retrieved. For $\epsilon \neq 0$, the system reaches the NESS; this state cannot be characterized using the Boltzmann distribution, and the numerical results are consistent with the exact solution. For instance, for $\epsilon = \{-2, 2\}$, the averaged output layer prediction is (i) $T_c(\epsilon = -2) \approx 1.3769$, and (ii) $T_c(\epsilon = +2) \approx 3.1071$. These results of $T_c(\epsilon)$ are close to the values of $T_c \approx 1.4182$ ($T_c \approx 3.1201$), obtained with Eq. (7). The discrepancy is mainly related to the role of unchanged energy $\Delta E = 0$ in the modified update rule when we generate the configurations, while this $\Delta E = 0$ is reasonably neglected in our calculation, see Eq. (12). In Table 1, we have provided a summary of the values of $T_c(\epsilon)$ that were obtained using the modified Metropolis method by means of MC simulations (literature), and supervised machine learning (our study). As summarized in this table, we see that MC and ML results are almost in agreement with each other. This explains the best performance of ML methods that CNN has the potential to exhibit phases and the transition temperature in unexplored out-of-equilibrium systems as well.

Parameter ϵ	$T_c(\epsilon)$ Exact (This Work) Eq. (7)	Machine Learning T_c^{ML} (This Work)	Monte Carlo T_c^{MC} Ref. [34]
0	$2/\ln(1+\sqrt{2}) \approx 2.2692$	2.2687(15)	—
-2	$5/4\ln(1+\sqrt{2}) \approx 1.4182$	1.3769(87)	1.3604(3)
+2	$11/4\ln(1+\sqrt{2}) \approx 3.1201$	3.1071(175)	3.1267(4)

Table 1: A summary of the values of transition temperature $T_c(\epsilon)$ for $\epsilon = \pm 2$ computed via supervised ML compared with exact result as well as the MC result reported in [34]. In our study, the equilibrium transition $T_c(\epsilon = 0)$ is used for validation. The error estimates are given in parentheses.

In conclusion, CNN is easily programmable using more convoluted software libraries, and it can be advanced to identify the non-equilibrium phase transitions from typical raw lattice configurations generated by the modified Metropolis MC simulations. Investigating whether or not this numerical method can be extended to the non-equilibrium phase transitions in an active spherical model is one of the fascinating questions that might be asked in this area. The spherical model is another model that can be exactly solved. In practice, it is used to characterize a wide variety of critical phenomena, including the ferromagnetic transition and the Bose-Einstein condensation, for example.

In this particular piece of work, we focused solely on the model's *static* characteristics. It has come to the attention of the authors that the parameter ϵ has been included here to only play the role of violating the DBC. In a remarkable turn of works, the subsequent focus of our research will be on the mathematical formalization as well as its complete physical description. Therefore, investigating the *dynamical* features of the models that violate DBC signifies a more intriguing potential course of the future direction.

Acknowledgements

Mulugeta Bekele and DW would like to thank International Science Programme, Uppsala, Sweden for the support not only in providing the facilities of Computational and Statistical Physics lab but also in covering all our travel as well as local expenses in visiting Indian Institute of Science, Bangalore, India. DW would like to thank Addis Ababa University and Dire Dawa University for financial support during his research work.

References

- [1] Kardar, M. *Statistical Physics of Fields*, Cambridge: Cambridge University Press, **2007**.
- [2] Nishimori, H.; Ortiz, G. *Elements of Phase Transitions and Critical Phenomena*, Oxford University Press: New York, **2011**.
- [3] Goldenfeld, N. *Lectures on Phase Transitions and The Renormalization Group*, CRC Press: Boca Raton, FL, **2018**.
- [4] Derrida, B. Non-equilibrium steady states: Fluctuations and large deviations of the density and of the current. *J. Stat. Mech.* **2007**, P07023.

- [5] Derrida, B. Microscopic versus macroscopic approaches to non-equilibrium systems. *J. Stat. Mech.* **2011**, P01030.
- [6] Bertini, L.; De Sole, A.; Gabrielli, D.; Jona-Lasinio, G.; Landim, C. Macroscopic fluctuation theory. *Rev. Mod. Phys.* **2015**, 87, 593.
- [7] Godreche C.; Bray, A.J. Nonequilibrium stationary states and phase transitions in directed Ising models. *J. Stat. Mech.* **2009**, P12016.
- [8] Stinchcombe, R. Stochastic non-equilibrium systems. *Adv. Phys.* **2010**, 50, 431.
- [9] Mukamel, D. Nonequilibrium Dynamics, Metastability and Flow. In *Soft and Fragile Matter*; Edited by Cates, M. E., Evans, R., CRC Press: Boca Raton, FL, **2000**, p. 237.
- [10] Odor, G. Universality classes in nonequilibrium lattice systems. *Rev. Mod. Phys.* **2004**, 76, 663
- [11] Hinrichsen, H. Non-equilibrium critical phenomena and phase transitions into absorbing states. *Advances in Physics*, **2000**, 49:7, 815.
- [12] Alpaydin, E. *Introduction to Machine Learning*, 4th ed; MIT Press: Cambridge, Massachusetts, 2004.
- [13] Tanaka, A.; Tomyia, A. Detection of phase transition via convolutional neural networks. *J. Phys. Soc. Jpn.* **2017**, 86, 063001
- [14] Walker, N.; Tam, K. M.; Novak, B.; Jarrell, M. Identifying structural changes with unsupervised machine learning methods. *Phys. Rev. E* **2018**, 98, 053305
- [15] Alexandrou, C.; Athenodorou, A.; Chrysostomou, C.; Paul, S. The critical temperature of the 2D-Ising model through Deep Learning Autoencoders. *Eur. Phys. J. B* **2020**, 93, 226
- [16] Burak, C.; Romer Rudolf, A.; Andreas Honecker. Machine Learning the Square-Lattice Ising Model. *J. of Physics: Conf. Series*. **2022**, 2207, 012058.
- [17] Huembeli, P.; Dauphin, A.; Wittek, P. Identifying quantum phase transition with adversarial neural networks. *Phys. Rev. B* **2018**, 97, 134109.
- [18] Dong, X. Y.; Pollmann, F.; Zhang, X F. Machine learning of quantum phase transitions. *Phys. Rev. B* **2019**, 99, 121104.
- [19] Ohtsuki, T.; Ohtsuki, T. Deep Learning the Quantum Phase Transitions in Random Two-Dimensional Electron Systems. *J. Phys. Soc. Jpn.* **2016**, 85, 123706
- [20] Ohtsuki, T.; Mano, T. Drawing Phase Diagrams of Random Quantum Systems by Deep Learning the Wave Functions. *J. Phys. Soc. Jpn.* **2020**, 89, 022001
- [21] Pilania, G.; Wang, C.; Jiang, X.; Rajasekaran, S.; Ramprasad, R. (2013) Accelerating materials property predictions using machine learning. *Sci. Rep.* **2013**, 3, 2810
- [22] Onsager, L. Crystal Statistics. I. A two Dimensional Model with an Order-Disorder Transition. *Phys. Rev.* **1944**, 65, 117-149
- [23] Yang, C.N.; Lee, L.D. Statistical theory of equations of state and phase transitions:I. Theory of condensation. *Phys. Rev.*, **87**: 404, 1952.
- [24] Lee, L.D.; Yang, C.N. Statistical theory of equation of state and phase transition: II. Lattice gas and Ising model. *Phys. Rev.*, **87**: 410, 1952.
- [25] Morningstar, A.; Melko, R. G. (2018) Deep Learning the Ising Model Near Criticality. *J. Mach. Learn. Res.* **2018**, 18, 1-17
- [26] Walker, N.; Tam, K. M.; Jarrell, M. Deep learning on the 2-dimensional Ising model to extract the crossover region with a variational autoencoder. *Sci. Rep.* **2020**, 10, 13047.
- [27] D'Angelo, F.; Böttcher, L. Learning the Ising Model with Generative Neural Networks. *Phys. Rev. Research* **2020**, 2, 023266.
- [28] Carrasquilla, J.; Melko, R. G. Machine learning phases of matter. *Nat. Phys.* **2017**, 13, 431-434.
- [29] Corte, I.; Acevedo, S.; Arlego, M.; Lamas, C. Exploring neural network training strategies to determine phase transitions in frustrated magnetic models. *Comput. Mater. Sci.* **2021**, 198, 110702.
- [30] Acevedo, S.; Arlego, M.; Lamas, C. A. Phase diagram study of a two-dimensional frustrated antiferromagnet via unsupervised machine learning *Phys. Rev. B* **2021**, 103, 134422.
- [31] Zhenyu Li; Mingxing Luo; Xin Wan. Extracting critical exponents by finite-size scaling with convolutional neural networks, *Phys. Rev. B*, **2019**, 99, 075418.

- [32] Burzawa, L.; Liu, S.; Carlson, E. W. (2019) Classifying surface probe images in strongly correlated electronic systems via machine learning, *Phys. Rev. Materials*, **3**, 033805
- [33] Bahri, Y. *et al.* Statistical Mechanics of Deep Learning. *Annu. Rev. Condens. Matter Phys.* **2020**: 11, 501-28
- [34] Kumar, M.; Dasgupta, C. Nonequilibrium phase transition in an Ising model without detailed balance. *Phys. Rev. E*. **2020**, 102, 052111.
- [35] Berg, B. *Markov Chain Monte Carlo Simulations and their Statistical Analysis with Web-Based Fortran Code*; World Scientific Publishing Company: 2004.
- [36] Landau, D. P.; Binder, K. *A Guide to Monte Carlo Simulations in Statistical Physics*, 4th ed.; Cambridge University Press, 2014.
- [37] Metropolis, N.; Rosenbluth, A. W.; Rosenbluth, M. N.; Teller, A. H.; Teller, E. Equation of State Calculations by Fast Computing Machines. *J. Chem. Phys.* **1953**, 21, 1087-1092.
- [38] Janke, W. *Introduction to Simulation Techniques*, Lect. Notes Phys. 716; Springer-Verlag: Berlin Heidelberg, **2007**, pp. 207-260.
- [39] Abadi, M. *et al.* TensorFlow: Large-scale machine learning on heterogeneous systems, 2015.
- [40] McCoy, B.M.; Wu, T.T. *The two-dimensional Ising model*, Harvard University Press: Cambridge, Massachusetts, 1973.
- [41] Glauber, R. J. Time-Dependent Statistics of the Ising Model. *J. Math. Phys.* **1963**, 4, 294.
- [42] Zia, R.K.P.; Schmittmann, B. Probablity currents as principal characterstics in the statistical mechanics of non-equilibrium steady states. *J. Stat. Mech.* **2007**, P07012.
- [43] For $\varepsilon \geq 8$ DBC is satisfied though at an effective temperature $T_{\text{eff}} = T/2$ and, therefore, the critical temperature at which an *equilibrium* transition takes place is given by $T_c(\varepsilon \geq 8) = 2T_c^0$, where $T_c^0 = T_c(\varepsilon = 0)$ is the critical temperature of the nearest-neighbor equilibrium Ising model on a square lattice. Respectively, DBC is satisfied for $\varepsilon \leq -8$ in the limit of $T_{\text{eff}} \rightarrow \infty$, implying that the system is effectively at an infinite temperature for all T and there is *no phase transition* [34].
- [44] The schematic diagram was adapted from draw-convnet, 2017.
- [45] Hinton, G.; Srivastava, N.; Krizhevsky, A.; Sutskever, I.; Salakhutdinov, R. Improving neural networks by preventing co-adaptation of feature detectors, 2012.
- [46] Dagne, W.T; Mulugeta, B. *A Comprehensive Study in Preparation*.

A Appendix (Supplementary Page)

A.1 Graphical Solution to $T_c(\varepsilon)$ Eq. (7)

Make use of the transition rate for flipping a spin ($\sigma_i \rightarrow -\sigma_i$), Eq. (5), and the basic definition of the energy change, $\Delta E = \{-8, -4, 0, 4, 8\}$, it is important to consider the following two main cases:

(i) First one can simply verify that the modified algorithm (5) still satisfies the DBC when $|\varepsilon| \geq 8$. This can be described as follows.

a) Assume for $\varepsilon \geq 8$ which implies that $\varepsilon \pm \Delta E \geq 0$. Subsequently, the transition rates are

$$W(\sigma_i \rightarrow -\sigma_i) = e^{-(\Delta E + \varepsilon)/T}, \text{ and } W(-\sigma_i \rightarrow \sigma_i) = e^{-(\Delta E - \varepsilon)/T},$$

where the ratio becomes

$$w(\varepsilon \geq 8) = e^{-2\Delta E/T}. \quad (8)$$

Therefore, this satisfies the DBC; though at an effective temperature $T_{\text{eff}} = T/2$. As a result, the *equilibrium* transition temperature equals $T_c(\varepsilon \geq 8) = 2T_c^0$, where $T_c^0 = T_c(\varepsilon = 0)$ refers to the transition temperature of this model [22].

b) If we consider $\varepsilon \leq -8$, it follows that $\varepsilon \pm \Delta E \leq 0$ meaning that $W(\sigma_i \rightarrow -\sigma_i) \equiv W(-\sigma_i \rightarrow \sigma_i) = 1$, with the ratio $w(\varepsilon \leq -8) = 1$. Thus, the DBC is satisfied in this case within the limit that $T_{\text{eff}} \rightarrow \infty$, indicating that there is *no phase transition* [43].

(ii) Now the second case ($|\varepsilon| < 8$) breaks the DBC since it is impossible to obtain a unique T_{eff} in which the transition probabilities of the given ΔE can respect the DBC. We can explain this as shown below.

a) Let we consider $0 < \varepsilon < 8$. It follows that,

$$\underbrace{W(\sigma_i \rightarrow -\sigma_i) = e^{-(\Delta E + \varepsilon)/T}, \text{ and } W(-\sigma_i \rightarrow \sigma_i) = \min \left[1, e^{-(\Delta E - \varepsilon)/T} \right]}_{\text{for } \Delta E > 0} \quad (9)$$

and

$$\underbrace{W(\sigma_i \rightarrow -\sigma_i) = \min \left[1, e^{-(\Delta E + \varepsilon)/T} \right], \text{ and } W(-\sigma_i \rightarrow \sigma_i) = e^{-(\Delta E - \varepsilon)/T}}_{\text{for } \Delta E < 0} \quad (10)$$

Here, in both (9 and 10), the ratio of the transition probabilities is subject to the value of ΔE , implying that it is impossible to find a unique value of T_{eff} . If a phase transition occurs, then the value of T_c must satisfy $T_c^0 < T_c < 2T_c^0$.

b) If we follow the same arguments for $-8 < \varepsilon < 0$, it can be inferred that T_c is expected to be in the interval $0 < T_c < T_c^0$.

Recall the definition of the energy change within the *equilibrium* Ising model that, $\Delta E = \{-8, -4, 0, 4, 8\}$. It can be noted from Ref. [34] that, $T_c = 0$ for $\varepsilon \leq \Delta E_{\min} = -8$, it increases from 0 with increasing ε from -8 to $\Delta E_{\max} = 8$, and becomes $2T_c^0$ for $\varepsilon \geq \Delta E_{\max}$. Explicitly, as required for the purpose of this work, we are essentially interested in some ε values lie in $-8 < \varepsilon < 8$, see Figure 4. For this ε values, $T_c(\varepsilon, \Delta E)$ can be discussed as follows. With positive $\Delta E = \{4, 8\}$, from Eq. (9), assume the case $W(-\sigma_i \rightarrow \sigma_i) = 1$ and hence the ratio becomes $\exp[-(\Delta E + \varepsilon)/T]$. Comparing this to that of the equilibrium case ($\varepsilon = 0$) at temperature T^0 , one can obtain $T\Delta E = T^0(\Delta E + \varepsilon)$. Similarly, for negative $\Delta E = \{-4, -8\}$, from (10) we find $T\Delta E = T^0(\Delta E - \varepsilon)$. As a result

$$T\Delta E = \begin{cases} T^0(\Delta E + \varepsilon), & \text{for } \Delta E > 0; \\ T^0(\Delta E - \varepsilon), & \text{for } \Delta E < 0. \end{cases} \quad (11)$$

This Eq. (12) allows us to relate a temperature $T(\varepsilon \neq 0)$ to $T(\varepsilon = 0)$. Since this relation provides different values for different ΔE , it is impossible to uniquely map the probability distribution in the NESS to the equilibrium distribution at a given T^0 . To get a unique result of T_c , we need to find the average over its different values obtained by using the possible values of $|\Delta E| = \{4, 8\}$. At the transition point, Eq. (12) implies that $T_c\Delta E = T_c^0(\Delta E \pm \varepsilon)$. We can write in its simple form as

$$T_c(\varepsilon, \Delta E) = \left(\frac{|\Delta E| + \varepsilon}{|\Delta E|} \right) T_c^0, \quad (12)$$

where $\Delta E \neq 0$ and $T_c^0 = 2/\ln(1 + \sqrt{2})$. The possible values of T_c in Eq. (12) for $\Delta E = \{-8, -4, 4, 8\}$ are shown in Figure 4(a). In order to obtain a unique value of T_c , we need to calculate the average over the different values of

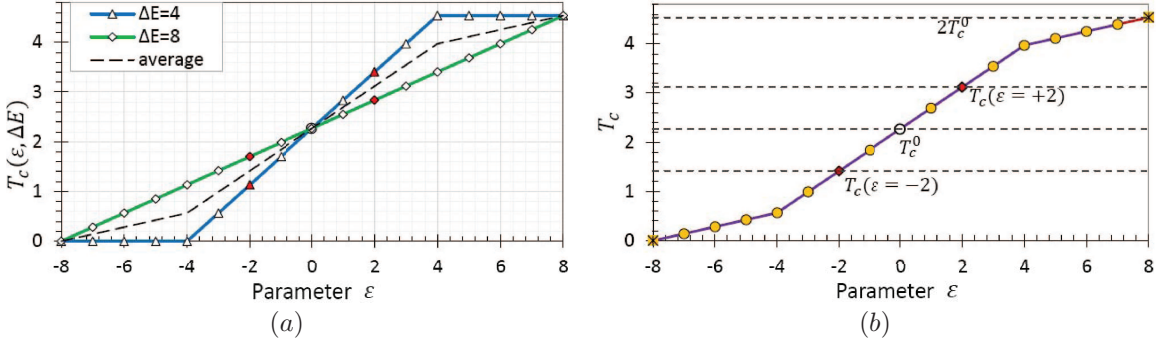


Figure 4: Critical temperature T_c as a function of parameter ε . (a) Plot of Eq. (13) with varying ΔE (see keys). The dashed line at the middle is equal to average of T_c for two ΔE values. (b) Plot of Eq. (7) and this is the same as the average T_c shown in "a". The horizontal dashed lines are $2T_c^0 \approx 4.5384$, $T_c(\varepsilon = +2) \approx 3.1201$, $T_c^0 \approx 2.2692$ and $T_c(\varepsilon = -2) \approx 1.4182$.

T_c that can be found from different choices of ΔE ². Accordingly, we can use Eq. (13) to get the exact solution that

²As a matter of fact only $\Delta E = \{4, 8\}$ can be used.

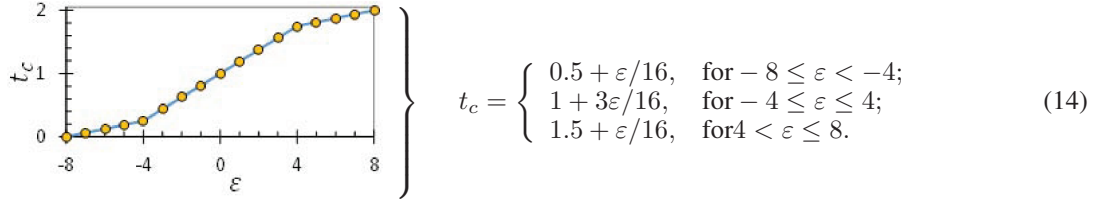
$$T_c^{\text{exact}}(\varepsilon) = (1 + 3\varepsilon/16)T_c^0 \text{ (for } -4 \leq \varepsilon \leq 4\text{), or}$$

$$T_c^{\text{exact}}(\varepsilon) = \frac{8 + \varepsilon}{8 \ln(1 + \sqrt{2})}, \text{ for } -8 \leq \varepsilon < -4; \quad (13a)$$

$$T_c^{\text{exact}}(\varepsilon) = \frac{16 + 3\varepsilon}{8 \ln(1 + \sqrt{2})}, \text{ for } -4 \leq \varepsilon \leq 4; \quad (13b)$$

$$T_c^{\text{exact}}(\varepsilon) = \frac{24 + \varepsilon}{8 \ln(1 + \sqrt{2})}, \text{ for } 4 < \varepsilon \leq 8. \quad (13c)$$

Alternatively, one can use $t_c = T_c/T_c^0$ to rewrite as



Implicitly, it can be inferred from Figure 4(b) that Eq. (13b) is efficient to discuss the non-equilibrium phase transition, where $T_c(\varepsilon = 0) = T_c^0$ and $t_c^0 = 1$.

A.2 Schematic Representation of the Modified Metropolis MC Simulation

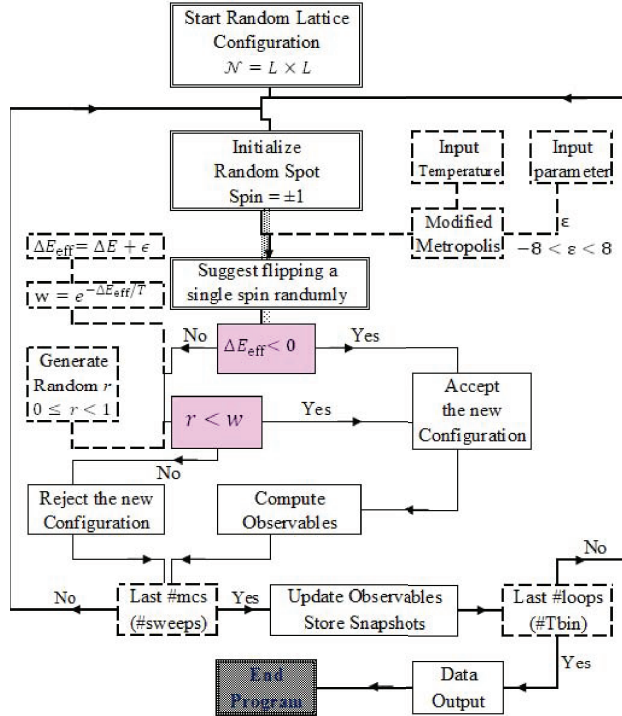


Figure 5: An schematic representation of the modified Metropolis MC simulation ($\Delta E_{\text{eff}} = \Delta E + \varepsilon$). First initialize a random configuration of $L \times L$ spins, then randomly choose a spin site to flip. Next compute ΔE_{eff} (4) where ΔE is readily from definition, if $\Delta E_{\text{eff}} < 0$ accept the flip, otherwise accept the flip with probability $w = e^{-\Delta E_{\text{eff}}/T}$. This is numerically implemented by generating a random number $r = [0, 1]$, if $r < w$ accept the flip and reject otherwise. We perform a sweep over the entire lattice of $N = L \times L$ spins 10 times, such that there is a total number of $10N$ possible spin flips to improve the generation of steady state data. Note that we recover the original Metropolis when $\varepsilon = 0$.

Representative Spin Configurations

Figure 6 demonstrates a system size of 30×30 representative Ising spin configurations at various values of temperature. There are 12 samples from the training (a) and 24 samples are from test datasets (b and c).

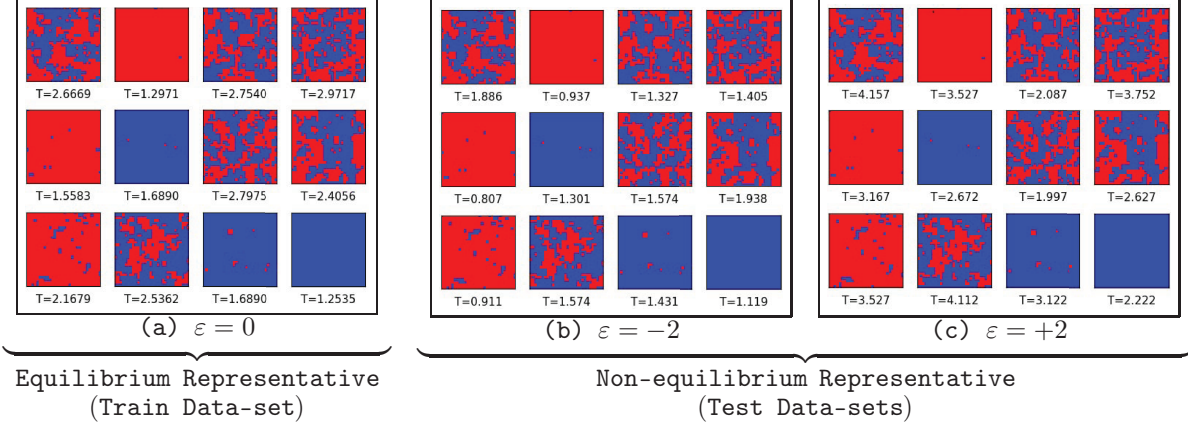


Figure 6: Representative spin configurations (30×30) from the training (panel a), and test (panels b and c) datasets. The low temperature ($T < T_c(\varepsilon)$) configurations tend to be predominately aligned in either the "down" (red) or "up" (blue) directions.

A.3 Architecture of Convolutional Neural Network

We build a simple convolutional neural network (CNN), implemented with TensorFlow [39] keras sequential model, to perform supervised machine learning (ML) on the Ising spin configurations sampled by the (effective) Metropolis MC simulation. An example of the architecture [44] of our model is represented as illustrated in Figure 7. As shown

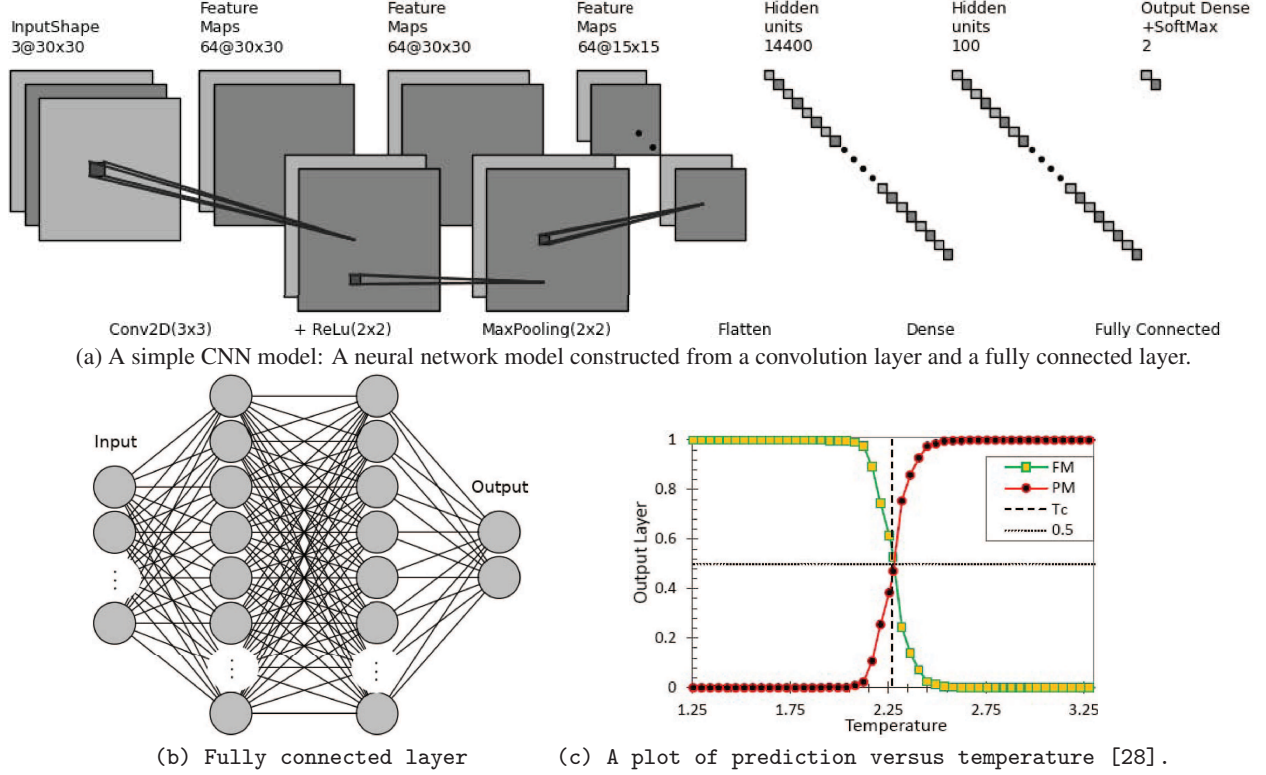


Figure 7: Schematic diagram of the machine learning architecture [44](an example).

in this example, the input layer consists of a square lattice ($L \times L$) Ising spin configurations. The input-shape specified on the input layer represents the shape of our input data (i.e., snapshot images). Here, the example with $L = 30$ shows that each image is 30 pixels wide and 30 pixels high, and has three (RGB) color channels which gives us an Inputshape = (30, 30, 3). In this model, the first hidden layer is a two dimensional convolutional layer (Conv2D_1). This layer has 64 output filters (each of 3×3 kernel size) with a single stride (Stride = 1), and we use rectified linear unit (ReLU) activation function. In addition, specifying padding and enabling the valid periodic-padding helps to account periodic boundary conditions. Note that the choice for the kernel size of 3×3 is generally a very common size to use, but the chosen number of output filters specified is arbitrary. One can choose different values of these parameters through observations during training the model of interest.

Next we add a second Conv2D_2 with the same specs as the first Conv2D_1. Similar to Conv2D_1, this Conv2D_2 has also 64 filters. Note also the choice of 64 here is arbitrary, even though having more filters in the later layers than in earlier layers is usually recommended in some cases. Optionally, one can add a max-pooling layer (MaxPool2D) to pool and reduce the dimensionality of the data³. Finally, we need to flatten the output from the convolutional layer and pass it to a Dense layer. We use an appropriate number of epochs (e.g., epoch = 4) and apply a Dropout regularization in the Dense layer in order to avoid overfitting [45]. In our case, the last Dense layer has two nodes (Dense = 2) which means that one for each classes; namely FM and PM states. In addition, we use the Softmax activation function on the last Dense layer so that the output for each sample is a probability distribution over the outputs of each classes.

As an example, Figure 7(c) shows the *prediction* (by prediction we mean the average output values of the final Dense layer) for configurations of different temperatures T where $\varepsilon = 0$ was used here. The red (●) and the green (□) curves represent the average prediction of the FM and PM phases, respectively. Here, the sum of the two prediction should be $P_{\text{FM}} + P_{\text{PM}} = 1$. The temperature at which the two curves intersect indicates the temperature at which CNN switches between classifying configurations as ‘FM’ versus ‘PM’ phases. The crossing point is also known as point of maximal confusion (POM). The horizontal dashed line represents an estimate of prediction $P = 0.5$, while the vertical dashed line indicates the model’s crossing temperature T^* . (Note that these notations are also same for detail results presented in Sec. 3.) Remarkably, the value of T^* agrees with the exact result, $T^* \approx T_c^0$. For the detailed numerical analysis presented in section 3, we stick ourselves to $\varepsilon = \pm 2$. The example of qualitative dependence of the critical temperature T_c on ε is presented in A.4. To this end, a basic understanding of PT between the PM phase ($T > T_c$) and the FM phase ($T < T_c$), permits and helps our efforts to categorize the two different types of configurations via ML [28].

A.4 Qualitative Dependence of T_c on the Parameter ε

Figure 8 shows the plots of prediction versus T for $L = 30$ and for some values of ε to show the dependence of the

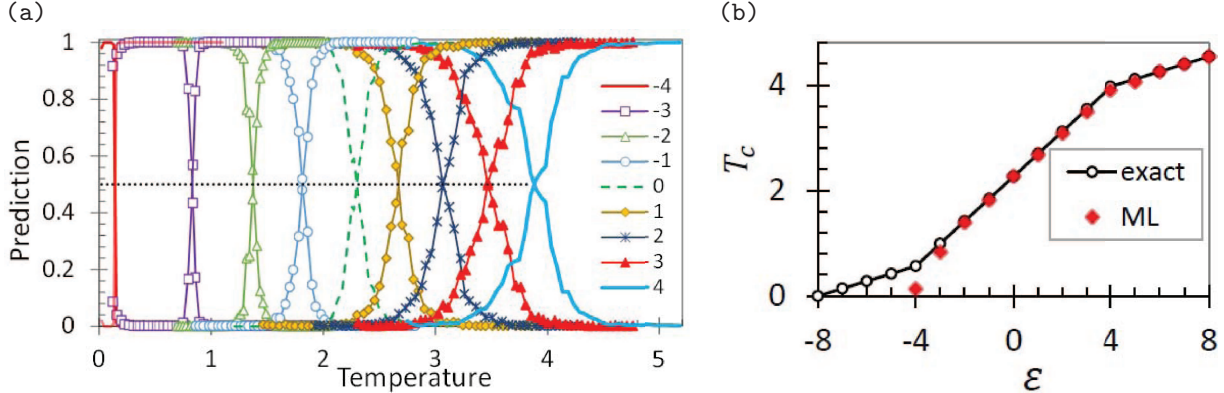


Figure 8: (a) Prediction versus temperature for various ε values. (b) Qualitative dependence of T_c on ε where we compare the numerical result of T_c^{ML} with that of the exact result T_c^{exact} .

critical temperature T_c on ε . The positions at which the curves are crossing each others give estimates of $T_c(\varepsilon)$. Notice the shifting of T_c to higher values with increasing ε . The inset of this figure shows a plot of $T_c(\varepsilon)$, estimated as the value of T at which curves cross, as a function of ε . For $\varepsilon = 0$, the model has an equilibrium phase transition at $T_c(\varepsilon = 0) \approx 2.2692$. It is clear from the plot in the inset that T_c approaches zero for large negative values of ε and it

³We use Ref. [12] for the fundamental understanding of max-pooling, padding, convolutional filters, and CNN

is $\simeq 2T_c(\varepsilon = 0)$ for $\varepsilon = 8$. This is in agreement with Eqs. (6) and (7) for $-4 < \varepsilon < 8$. However, the model fails to detect the transition temperature for $-8 < \varepsilon < -4$.

A.5 FSS of the Transition Temperature and the Critical Exponent (γ)

Figure 9 demonstrates the FSS analysis of the crossing temperature $T^*(L)$ as a function of $1/L$ for $L = \{10, 20, 30, 40, 60\}$. The horizontal red line (see keys) refers to the numerical T_c^{ML} (Table 1), and the magenta line represents T_c^{exact} (Eq. 13b).

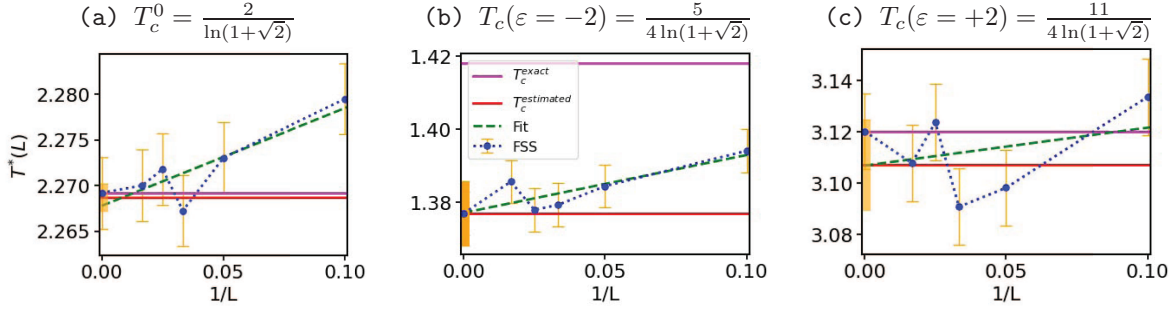


Figure 9: The crossing temperature $T^*(L)$ as a function of $1/L$. The horizontal red line (see keys) refers to the numerical T_c^{ML} (Table 1), and the magenta line represents T_c^{exact} (Eq. 13b) as shown in each ‘a’, ‘b’ and ‘c’.

line represents the critical temperature in thermodynamic limit that is calculated using Eq. (13b), $T_c(\varepsilon = \pm 2) = (16 + 3\varepsilon)/8\ln(1 + \sqrt{2})$, where the known result of $T_c(\varepsilon = 0)$ is shown for reference. The size of error bars is equal to one standard deviation statistical uncertainty⁴. The numerical results are (a) $T_c^{ML} \simeq 2.2687(15)$, (b) $T_c^{ML} \simeq 1.3769(87)$ and (c) $T_c^{ML} \simeq 3.1071(175)$.

The estimation of the critical exponent (γ) can be performed using the FSS theory $\chi \propto (T/T_c - 1)^{-\gamma}$ where χ represents the latent susceptibility [15]. If \tilde{z} denotes average absolute latent variable ($\tilde{z} = \langle |z| \rangle$), one can calculate χ as

$$\chi = \frac{\mathcal{N} (\langle \tilde{z}^2 \rangle - \langle \tilde{z} \rangle^2)}{T}, \quad (15)$$

recalling $\mathcal{N} = L \times L$ and defining $\tilde{z} = \frac{1}{M} \sum_{k=1}^M |z_k|$, where M is the total number of configurations and $k = \{1, \dots, M\}$. Figure 10 demonstrates the latent variable z as a function of T for the given configurations. As a result,

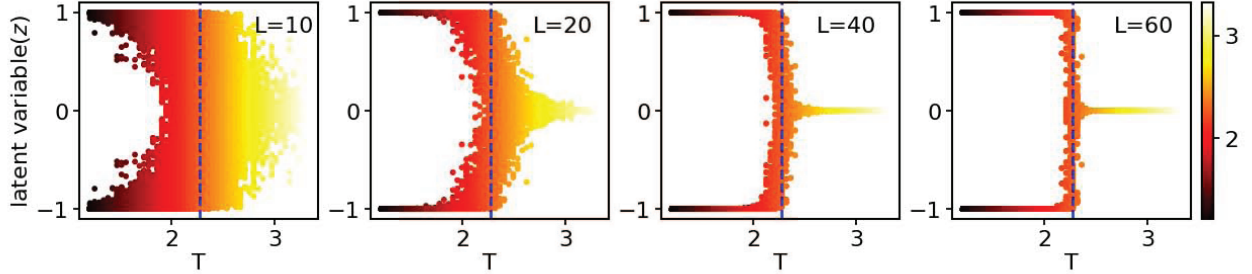


Figure 10: Scatter plots of the latent variable z versus T for four systems of each linear size L shown at the upper right. This is the case of equilibrium ($\varepsilon = 0$) model. The blue dashed line within each system denotes $T_c^0 = 2/\ln(1 + \sqrt{2})$. A gradient color at the right panel help to illustrates the temperature T and it reflects the nature of the phase diagram as we move from low T ($T < T_c^0$) to high T ($T > T_c^0$).

one can estimate γ using the result of Eq. 15 where \tilde{z} can be obtained from data presented in Figure 10 by plotting $\chi L^{-\gamma/\nu}$ versus $(T - T_c^0)L^{1/\nu}$.

Therefore, it is straightforward to apply this method to the nonequilibrium case ($\varepsilon \neq 0$). Figure 11 shows the latent variable z as a function of T (a) $\varepsilon = -2$ and (b) $\varepsilon = +2$. In fact, a comprehensive investigation of this topic is underway [46].

⁴See the supplementary material in Ref. [28]

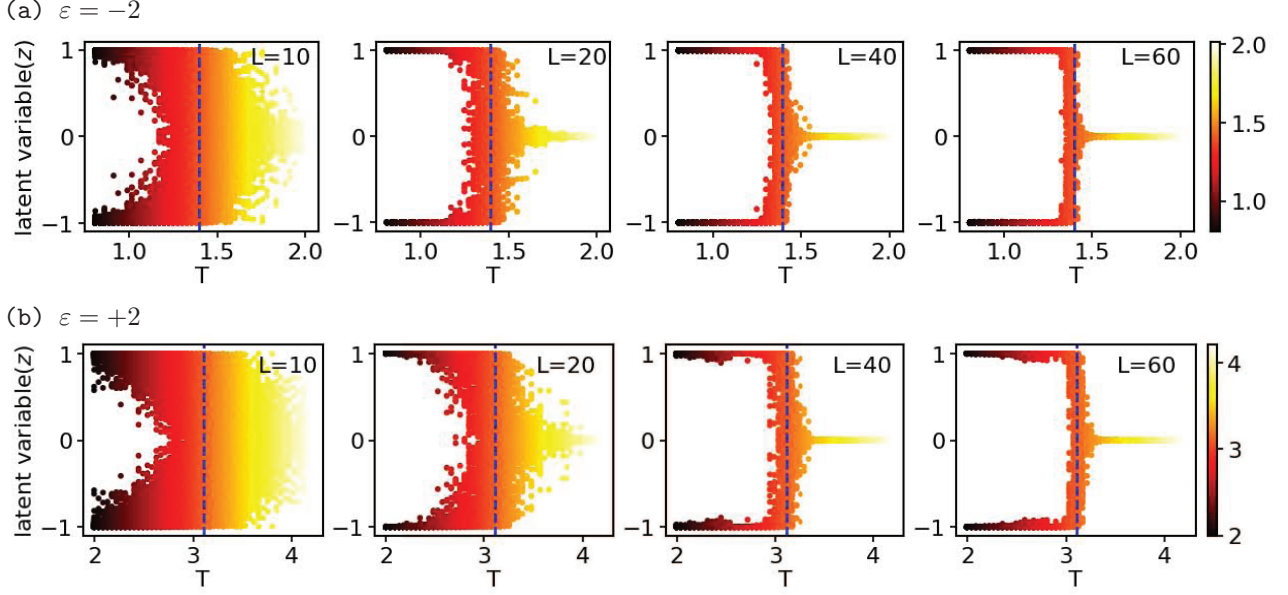


Figure 11: Scatter plots of the latent variable z versus T for the given linear size, $\varepsilon = -2$ (upper panel) and $\varepsilon = +2$ (lower panel). Here the blue dashed lines denote (a) $T_c(\varepsilon = -2) = (5/4)/\ln(1+\sqrt{2})$ and (b) $T_c(\varepsilon = -2) = (11/4)/\ln(1+\sqrt{2})$. The gradient color shown for each panel demonstrates the nature of the phase diagram from the low T ($T < T_c$) to the high T ($T > T_c$).

Abbreviations

CNN	Convolutional Neural Networks
DBC	Detailed Balance Condition
FM	Ferromagnetic
FSS	Finite Ssize Scaling
MC	Monte Carlo
ML	Machine learning
NESS	Non-equilibrium Steady States
PM	Paramagnetic
PT	Phase Transitions

Data Availability

The neural network result was calculated using TensorFlow [39] integrated with Keras environment. Required datasets are available from the authors for a reasonable request.